Taylor & Francis
Taylor & Francis Group

RESEARCH PAPER

Check for updates

Standardized uptake value (SUV$_{max}$) in ^{18}F-FDG PET/CT is correlated with the total number of main oncogenic anomalies in cancer patients

Amin Haghighat Jahromi [iD][a], Geraldine Chang[a], Razelle Kurzrock [iD][b], and Carl K. Hoh[a]

[a]Department of Radiology, University of California San Diego, La Jolla, CA, USA; [b]Center for Personalized Cancer Therapy and Division of Hematology and Oncology, Department of Medicine, University of California San Diego, Moores Cancer Center, La Jolla, CA, USA

ABSTRACT

Cancer diagnosis and therapy is quickly moving from the traditional histology-based approaches to genomic stratification, providing a huge opportunity for radiogenomics, associating imaging features with genomic data. Genome sequencing is time consuming, expensive and invasive whereas ^{18}F-FDG PET/CT is readily available, fast and noninvasive. The aim of this study was to determine the relationship between the maximum standardized uptake value (SUV$_{max}$) and the frequency of 11 common oncogenic anomalies determined by specific common genomic alterations in tissue biopsies from patients with cancer. We retrospectively studied 102 consecutive untreated patients with gastrointestinal, lung, and breast cancer who underwent ^{18}F-FDG PET/CT imaging, shortly prior to molecular testing by a biopsy for genomic profiling that consisted of 11 common DNA alterations: (1) TP53, (2) DNA repair, (3) EGFR, (4) PI3K/AKT/MTOR (PAM) pathway including PTEN, PIK3CA, AKT, TSC, CCNB1, MTOR, FBXW2, and NF2, (5) MEK, (6) CYCLIN including CCND,CDK, CDKN, and RB, (7) WNT, (8) ALK, (9) MYC, (10) MET, and (11) FGF/FGFR. Higher SUV$_{max}$ was associated with the presence of TP53 and PAM genomic anomalies ($p < .05$), but not the other 9 gene groups ($p > .05$). More importantly, SUV$_{max}$ was positively correlated with total number of oncogenic anomalies ($r = 0.27$, $p = .005$). We propose higher SUV$_{max}$ as an indicator for total number of common oncogenic anomalies. This finding is a step forward in noninvasive stratification of cancer patients, in terms of the overall load of oncogenic anomalies, based on their SUV$_{max}$.

Introduction

The relatively new field of cancer genome sequencing is changing the landscape of oncology.[1] Radiogenomics plays an important role by finding relationship and creating link between imaging profiles and genomics.[2] Radiogenomics has been used mainly in computer tomography (CT) and magnetic resonance imaging (MRI) to draw a link between imaging features and tumor genotypes.[3] However, radiogenomics in the field of nuclear medicine is not explored to the same extent, although ^{18}F-fluorodeoxyglucose positron emission tomography (^{18}F-FDG PET) is regularly used for cancer diagnosis and treatment follow up.[4–6] Standardized uptake value (SUV$_{max}$) is routinely used as a quantitative indicator of ^{18}F-FDG uptake, thus glucose metabolism rate (GMR). SUV$_{max}$ has been shown to correlate with P53 alterations and its relationship with a variety of genomic alteration has been studied previously; however, it remains mostly nonspecific at the molecular and genetic level.[7–9]

There are several common genomic anomalies that play role in tumorigenesis.[1] Determining the presence of each genomic alteration is necessary for targeted therapy. The total number of common oncogenic anomalies is also crucial information, as an indicator of the overall load of oncogenic anomalies.[10,11]

Increased SUV$_{max}$ is a hallmark of cancer. Although commonly explained as a result of increased proliferation rate, the genetic underpinning of increased SUV$_{max}$ in cancer is still not clearly understood.[12,13] Oncogenic anomalies are proposed to be associated with metabolic reprogramming in cancer cells, causing increased GMR; however, such an association has not yet been established, clinically.[14] In our prior study, we showed a potential relationship between SUV$_{max}$ and the number of genomic anomalies of the tumor; however, we analyzed only a small subset of patients ($N = 3$) at the two extremes of SUV$_{max}$.[13] Herein, we sought to study if higher total number of these genomic anomalies is associated with higher SUV$_{max}$, in the biopsied lesions. Genome sequencing is time consuming, expensive and invasive whereas ^{18}F-FDG PET/CT is readily available, fast and noninvasive. Our hypothesis is that the total number of oncogenic anomalies is related to SUV$_{max}$, in the biopsied lesion.

Results

Patients

We studied 102 untreated patients including 42 (41.2%) breast, 26 (25.5%) gastrointestinal, and 34 (33.3%) lung cancer patients. Due to the retrospective nature of this study, the patients were in different stages of their cancers and the lesion biopsied included primary or metastatic lesions.

CONTACT Amin Haghighat Jahromi ✉ ajahromi@ucsd.edu 🖃 Department of Radiology, University of California San Diego, 9300 Campus Point Dr., La Jolla, CA 92037

Associations between individual genes/gene families and SUV$_{max}$

Forty seven of the 102 patients (46%) had anomalies in TP53 and a significantly higher mean SUV$_{max}$ of 9.0 compare to patients with unaltered TP53 which had a mean SUV$_{max}$ of 6.3 ($p = .002$). Forty of the 102 patients (39%) had abnormalities in PAM pathway genes (PTEN, PIK3CA, AKT, TSC, CCNB1, MTOR, FBXW2, and NF2). The mean SUV$_{max}$ for these 40 patients was 8.7, significantly higher than 6.8 in patients without abnormal PAM pathway genes ($p = .042$).

Four of 102 patients (4%) had DNA repair gene (BRCA, BRIP, ATM, MMR, MSH, MLH) anomalies. The mean SUV$_{max}$ of these 4 patients was 9.7, not significantly different from 7.4 in those without DNA repair gene anomalies ($p = .28$). Twenty eight of 102 patients (27%) had EGFR gene anomalies. The mean SUV$_{max}$ of these 28 patients was 7.6, not significantly different from 7.5 in those without EFGR gene anomalies ($p = .98$). Eighteen of the 102 patients (18%) had abnormalities in MEK genes (RAS, RAF, MAPK, and CNAS). The mean SUV$_{max}$ for these 18 patients was 8.9, not significantly higher than 7.2 in patients without abnormal MEK pathway genes ($p = .16$). Thirty nine of the 102 patients (38%) had abnormalities in CYCLIN pathway genes (CCND, CDK, CDKN, RB) and a mean SUV$_{max}$ of 7.8 compared to 7.4 in the patient without CYCLIN abnormality. These means were not significantly different ($p = .68$). Seventeen of the 102 patients (17%) had abnormalities in WNT genes (APC, CTNNB, NOTCH) and a mean SUV$_{max}$ of 8.2 compared to 7.4 in the patient without WNT abnormality. These means were not significantly different ($p = .52$). Three of the 102 patients (3%) had abnormalities in ALK gene and a mean SUV$_{max}$ of 11.9 compared to 7.4 in the patient without ALK abnormality. These means were not significantly different ($p = .09$). Fourteen of the 102 patients (14%) had MYC gene anomalies and a corresponding mean SUV$_{max}$ of 8.7, not significantly different compared to the 88 patients without MYC gene anomalies with a mean SUV$_{max}$ of 7.4 ($p = .31$). Two of the 102 patients (2%) had MET gene anomalies and a corresponding mean SUV$_{max}$ of 6, not significantly different compared to the 100 patients without MET

gene anomalies with a mean SUV$_{max}$ of 7.6 ($p = .63$). Twenty one of the 102 patients (21%) had FGF/FGFR gene anomalies and a mean SUV$_{max}$ of 6.8 as compared to the 81 patient without anomalies and a mean SUV$_{max}$ of 7.7. This was not significant ($p = .40$).

Total number of main oncogenic anomalies

Total number of oncogenic anomalies from the aforementioned 11 genetic groups was calculated for each patient from summation of the individual genomic anomalies. This number actually ranged from 0 to 6, as no patient had more than 6 oncogenic anomalies. In fact, 12 patients (12%) had no genetic anomalies, 19 patients (19%) had 1 genetic alteration, 30 patients (29%) had 2 total anomalies, 17 patients (17%) had 3 total anomalies, 18 patients(18%) had total of 4 anomalies, 5 patients (5%) had total of 5 anomalies, and 1 patient (1%) had 6 oncogenic anomalies (Figure 1). No patient had more than 6 oncogenic anomalies. The SUV$_{max}$ was positively correlated to the total of oncogenic anomalies ($r = 0.27$, $p = .005$).

Discussion

Radiogenomics, defined as associating imaging features with genomic data, is gaining attention as the precision medicine is rapidly evolving.[15,16] 18F-FDG PET/CT is standard of care for cancer staging/restaging, to guide therapeutic decisions and monitor therapeutic response. In our prior study, we used a simple method where we ranked the patients based on SUV$_{max}$. Then we selected three patients with the highest SUV$_{max}$ and three patients with the lowest SUV$_{max}$, and speculated that the patients with the highest SUV$_{max}$ group had more genomic anomalies.[13] In the current study, we performed a rigorous statistical analysis of a more homogenous subset of the previous study population, containing only patients with breast, lung and gastrointestinal tumors. In addition, the analysis of the relationship between SUV$_{max}$ and total number of genetic anomalies was performed on all 102 patients. The aim of this study was to determine the relationship of the SUV$_{max}$
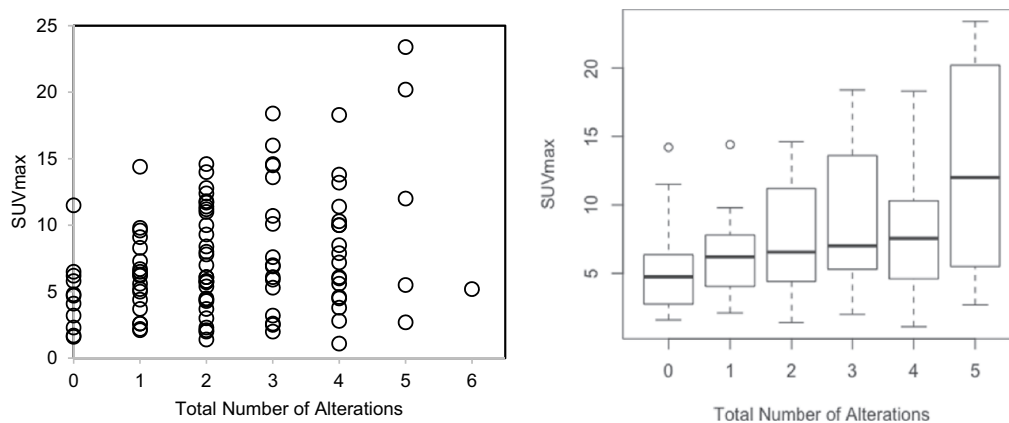
Figure 1. Relationship between SUV$_{max}$ and the total number of oncogenic alterations with Pearson correlation coefficient $r = 0.27$ ($p = .005$). Left panel shows the scatter plot of all patients ($n = 102$) with circles represent individual datapoints. Right panel shows the box plot for all patients excluding the group with 6 oncogenic alterations because there was only one patient in that group. The central thick black line indicates the median, and the bottom and top of the rectangle are the 25th (Q1) and 75th (Q3) percentiles. The circles represent outlier SUV$_{max}$, defined as either larger than Q3 + 1.5 × IQR or smaller than Q1 − 1.5 × IQR, where IQR = Q3 − Q1 is the interquartile range. The horizontal "whiskers" represent the largest and smallest non-outlier observations in the data set.

Table 1. Mean SUV$_{max}$ and number of patients with or without genomic alteration ($n = 102$).

| Gene | Mean SUV$_{max}$, number of patients | | p value |
	With genomic alteration	Without genomic alteration	
TP53	9.0 ($n = 47$)	6.3 ($n = 55$)	**0.002***
PAM	8.7 ($n = 40$)	6.8 ($n = 62$)	**0.042***
EGFR	7.6 ($n = 28$)	7.5 ($n = 74$)	0.98
MEK	8.9 ($n = 18$)	7.2 ($n = 84$)	0.16
CYCLIN	7.8 ($n = 39$)	7.4 ($n = 63$)	0.68
WNT	8.2 ($n = 17$)	7.4 ($n = 85$)	0.52
ALK	11.9 ($n = 3$)	7.4 ($n = 99$)	0.09
MYC	8.7 ($n = 14$)	7.4 ($n = 88$)	0.31
MET	6.0 ($n = 2$)	7.6 ($n = 100$)	0.63
FGF/FGFR	6.8 ($n = 21$)	7.7 ($n = 81$)	0.40

*Among 11 common oncogenic alterations, only TP53 and PAM alterations were significantly related to SUV$_{max}$.

of the biopsied lesion, with the sum of 11 common oncogenic anomalies including *TP53, EGFR, ALK, MYC, MET, FGF/ FGFR*, DNA repair, PI3K/Akt/mTOR (PAM), MEK, CYCLIN, and WNT determined by specific common genomic anomalies in tissue biopsies from breast, gastrointestinal and lung cancer patients. Our speculation was that higher number of total oncogenic anomalies cause metabolic reconfiguration,[14] thus increased GMR and SUV$_{max}$.

SUV$_{max}$ was positively correlated to the total number of oncogenic anomalies ($r = 0.27$, $p = .005$), in the biopsied lesion (Figure 1). The SUV$_{max}$ was also positively correlated with TP53, as previously shown,[13] and also with PAM anomalies (Table 1). Relationship between SUV$_{max}$ and other 9 individual oncogenic abnormalities, individually, was not statistically significant (Table 1). Representative images from two patients with total number of oncogenic anomalies of 0 and 5 and respective SUV$_{max}$ of 4.9 and 23.6 are shown (Figures 2 and 3).

Our finding suggests that higher SUV$_{max}$ is an indicator of total number of oncogenic anomalies. We speculate that higher

Figure 2. FDG PET projection image in a patient with adenocarcinoma of the lung. The biopsied right lung hypermetabolic lesion had SUV$_{max}$ of 20.2 (arrow). This lesion had a total number of main oncogenic alterations of 5.

number of oncogenic anomalies cause metabolic reprogramming by stimulating glucose uptake, and channeling glucose to aerobic glycolysis,[14,17,18] therefore increase SUV$_{max}$. We suggest that SUV$_{max}$ merits further study as an accessible and noninvasive surrogate for the total number of oncogenic anomalies derived from sequencing a tissue biopsy.

This study had several limitations including its retrospective nature, relatively small number of patients, and lack of a definite underlying mechanism. Also, the imaging and molecular testing were not exactly concurrent, because of the retrospective nature of the study.

Conclusions

^{18}F-FDG PET/CT SUV$_{max}$ is positively correlated with total number of oncogenic anomalies ($r = 0.27$, $p = .005$). This finding suggests that SUV$_{max}$ can estimate the total number of oncogenic anomalies, noninvasively. Since mutational load has been implicated as a predictive factor for immunotherapy response,[1,9]

Patients and methods

Patient selection

We studied 102 consecutive untreated patients including 42 breast, 26 gastrointestinal and 34 lung cancer patients who underwent 18F-FDG PET/CT, within six months before a biopsy for genomic profiling, a subpopulation of our prior work[13]. A 6-month cutoff was chosen to avoid a false positive or a false negative SUV$_{max}$ secondary to post-biopsy

Figure 3. FDG PET projection image in a patient with adenocarcinoma of the lung. The biopsied right lung hypermetabolic lesion had SUV$_{max}$ of 4.9 (arrow). This lesion had a total number of main oncogenic alterations of 0.

inflammatory changes or long time-lapse, respectively. Although concurrent imaging and molecular testing is ideal, the retrospective nature of this study precluded achieving concurrent imaging and molecular testing. Genomic profiling included 11 common DNA anomalies: (1) TP53, (2) DNA repair, (3) EGFR, (4) PI3K/AKT/MTOR (PAM) pathway including PTEN, PIK3CA, AKT, TSC, CCNB1, MTOR, FBXW2, and NF2, (5) MEK, (6) CYCLIN including CCND, CDK, CDKN, and RB, (7) WNT, (8) ALK, (9) MYC, (10) MET, and (11) FGF/FGFR. This study was performed in accordance with the guidelines of the UCSD Internal Review Board (PREDICT [Profile Related Evidence Determining Individualized Cancer Therapy], protocol; NCT02478931).

^{18}F-FDG PET-CT imaging

All patients were asked to fast for at least six hours prior to their scan. Blood glucose levels were measured immediately before the FDG injection and no patient had a blood glucose level >160 mg/dl. Patients were intravenously injected with 370–740 MBq FDG, within a 5–10 second interval. Following an uptake period of approximately 1 hour in a quiet room at rest, a multi-station 3-dimensional (3D) whole body PET acquisition with CT, for attenuation correction, was performed for approximately 60 min, using a GE Discovery VCT scanner (GE, Waukesha, WI). Whole-body CT covers a region ranging from the head to the mid-thigh. PET images were acquired, after the CT scan, at a rate of 2 minutes/bed position, in the 3D acquisition mode. CT images were then reconstructed onto a 512 × 512 matrix. PET images were reconstructed using a standard whole-body 3D iterative reconstruction: 2 iterations; 28 subsets onto a 128 × 128 matrix with attenuation correction, decay correction, and scatter correction. The photon energy window was 425–650 keV. Slice thickness was 3.27 mm and reconstruction diameter was 70 cm. Pixel size was 5.47 mm × 5.47 mm with spatial resolution of 5 mm. ^{18}F-FDG PET/CT images were generated for review on a workstation.

Image analysis

All PET images were reviewed and further analyzed on the institution's pictures archiving and communication system (PACS), (AGFA Impax 6.3, Mortsel Belgium) by a board certified academic nuclear medicine physician. The lesions that were later biopsied were selected for imaging analysis. Focal activities of the biopsied lesions were manually identified on PET images. SUVs of the biopsied lesions were obtained by manually placing a circular region of interest (ROI) at the site of the maximum FDG uptake in the PET images and the maximal activity (SUV_{max}) was recorded. SUV was calculated as decay-corrected activity of tissue volume (kBq/mL)/injected FDG activity per body mass (kBq/g).

Genomic analysis

Genomic analysis was performed on the biopsy samples, using a clinical next generation sequencing (NGS) based assay (182 to 315 genes) (FoundationOne™, Foundation Medicine Inc., Cambridge, MA), to interrogate for DNA alterations including detection of base substitutions, insertions, deletions, copy number alterations, and selected gene fusions in 11 classes of genomic pathways: *TP53, EGFR, ALK, MYC, MET, FGF/FGFR*, DNA repair, PI3K/Akt/mTOR (PAM), MEK, CYCLIN, and WNT pathway genes were analyzed.

Statistical analysis

Statistical analysis was done in R, version 3.5.2 and Microsoft Excel. Differences between SUV_{max} in oncogene positive versus negative group patients were analyzed by the paired *t*-test (two-tailed) and considered to be significant at a *p* value less than 0.05. The Pearson correlation coefficient (r) was used in the linear relationship between the SUV_{max} and total number of oncogenic anomalies.

Ethical approval and consent to participate

Disclosure of potential conflicts of interest

Funding

ORCID

Amin Haghighat Jahromi 🆔 http://orcid.org/0000-0002-8263-903X
Razelle Kurzrock 🆔 http://orcid.org/0000-0003-4110-1214

References

1. Vogelstein B, Papadopoulos N, Velculescu VE, Zhou S, Diaz LA, Kinzler KW. Cancer genome landscapes. Science. 2013;339:1546–1558.
2. Mazurowski MA. Radiogenomics: what it is and why it is important. J Am Coll Radiol. 2015;12:862–866. doi:10.1016/j.jacr.2015.04.019.
3. Jansen RW, van Amstel P, Martens RM, Kooi IE, Wesseling P, de Langen AJ, Menke-van der Houven van Oordt CW, Jansen BHE, Moll AC, Dorsman JC, et al. Non-invasive tumor genotyping using radiogenomic biomarkers, a systematic review and oncology-wide pathway analysis. Oncotarget. 2018;9(28):20134–20155. doi:10.18632/oncotarget.24893.
4. Dhingra VK, Mahajan A, Basu S. Emerging clinical applications of PET based molecular imaging in oncology: the promising future potential for evolving personalized cancer care. Indian J Radiol Imaging. 2015;25:332–341. doi:10.4103/0971-3026.169467.
5. Lee JW, Lee SM. Radiomics in oncological PET/CT: clinical applications. Nucl Med Mol Imaging. 2018;52:170–189. doi:10.1007/s13139-017-0500-y.

6. Suárez-Piñera M, Belda-Sanchis J, Taus A, Sánchez-Font A, Mestre-Fusco A, Jiménez M, Pijuan L. FDG PET-CT SUVmax and IASLC/ATS/ERS histologic classification: a new profile of lung adenocarcinoma with prognostic value. Am J Nucl Med Mol Imaging. 2018;8:100–109

7. Heiden BT, Chen G, Hermann M, Brown RKJ, Orringer MB, Lin J, Chang AC, Carrott PW, Lynch WR, Zhao L, et al. 18F-FDG PET intensity correlates with a hypoxic gene signature and other oncogenic abnormalities in operable non-small cell lung cancer. PLoS One. 2018;13(7):e0199970. doi:10.1371/journal.pone.0199970.

8. Nair VS, Gevaert O, Davidzon G, Napel S, Graves EE, Hoang CD, Shrager JB, Quon A, Rubin DL, Plevritis SK, et al. Prognostic PET 18F-FDG uptake imaging features are associated with major onco-genomic alterations in patients with resected non-small cell lung cancer. Cancer Res. 2012;72(15):3725–3734. doi:10.1158/0008-5472.CAN-11-3943.

9. Caicedo C, Garcia-Velloso MJ, Lozano MD, Labiano T, Vigil Diaz C, Lopez-Picazo JM, Gurpide A, Zulueta J, Richter Echevarria JA, Perez Gracia JL, et al. Role of [18F]FDG PET in prediction of KRAS and EGFR mutation status in patients with advanced non-small-cell lung cancer. Eur J Nucl Med Mol Imaging. 2014;41:2058–2065. doi:10.1007/s00259-014-2833-4.

10. Chalmers ZR, Connelly CF, Fabrizio D, Gay L, Ali SM, Ennis R, Schrock A, Campbell B, Shlien A, Chmielecki J, et al. Analysis of 100,000 human cancer genomes reveals the landscape of tumor mutational burden. Genome Med. 2017;9(1):34. doi:10.1186/s13073-017-0424-2.

11. Ock CY, Hwang JE, Keam B, Kim SB, Shim JJ, Jang HJ, et al. Genomic landscape associated with potential response to anti-CTLA-4 treatment in cancers. Nat Commun. 2017;8:1050.

12. Ahn KS, Kang KJ, Kim YH, Kim TS, Song BI, Kim HW, O'Brien D, Roberts LR, Lee JW, Won KS, et al. Genetic features associated with 18F-FDG uptake in intrahepatic cholangiocarcinoma. Ann Surg Treat Res. 2019;96:153–161. doi:10.4174/astr.2019.96.4.153.

13. Chang GH, Kurzrock R, Tran L, Schwaederle M, Hoh CK. mutations and number of alterations correlate with maximum standardized uptake value (SUVmax) determined by positron emission tomography/computed tomography (PET/CT). Oncotarget. 2018;9:14306–14310.

14. Choi H, Na KJ. Pan-cancer analysis of tumor metabolic landscape associated with genomic alterations. Mol Cancer. 2018;17:150. doi:10.1186/s12943-018-0895-9.

15. Ghasemi M, Nabipour I, Omrani A, Alipour Z, Assadi M. Precision medicine and molecular imaging: new targeted approaches toward cancer therapeutic and diagnosis. Am J Nucl Med Mol Imaging. 2016;6:310–327.

16. Vaidya T, Agrawal A, Mahajan S, Thakur MH, Mahajan A. The continuing evolution of molecular functional imaging in clinical oncology: the road to precision medicine and radiogenomics (Part I). Mol Diagn Ther. 2019;23:1–26. doi:10.1007/s40291-018-0366-4.

17. Hay N. Reprogramming glucose metabolism in cancer: can it be exploited for cancer therapy? Nat Rev Cancer. 2016;16:635–649. doi:10.1038/nrc.2016.77.

18. Granja S, Pinheiro C, Reis RM, Martinho O, Baltazar F. Glucose addiction in cancer therapy: advances and drawbacks. Curr Drug Metab. 2015;16:221–242.